CRITICAL RAW MATERIALS ELIMINATION BY A TOP-DOWN APPROACH TO HYDROGEN AND ELECTRICITY GENERATION

Grant agreement no.: 721065

***Start date**: 01.01.2017 – **Duration**: 42 months*

***Project Coordinator**: CNRS*

DELIVERABLE REPORT

DELIVERABLE 3.6 – CRM-FREE METAL@CARBON MATERIALS AS HER CATALYSTS: SYNTHESIS, CHARACTERIZATION AND PERFORMANCE IN BMEL	
Due Date	31/12/2020 (M48)
Author(s)	Tanja Kallio, Nana Han, Frédéric Jaouen, Björn Eriksson
Work Package	WP3: Catalyst synthesis and characterization
Work Package Leader	Tanja Kallio (AALTO)
Lead Beneficiary	AALTO
Date released by WP Leader	27/01/2021
Date released by Coordinator	27/01/2021

DISSEMINATION LEVEL		
PU	*Public*	***PU***
PP	*Restricted to other programme participants (including the Commission Services)*	
RE	*Restricted to a group specified by the consortium (including the Commission Services)*	
CO	*Confidential, only for members of the consortium (including the Commission Services)*	

NATURE OF THE DELIVERABLE		
R	*Report*	***R***
P	*Prototype*	
D	*Demonstrator*	
O	*Other*	

SUMMARY	
Keywords	hydrogen evolution reaction, acid media, electrocatalyst, catalyst, critical raw material
Full Abstract (Confidential)	In this report, we present the consortium's work on PGM-free and/or CRM-free catalysts for the hydrogen evolution reaction (HER) in acid media. Catalysts based on iron, nickel, iron-nickel, tungsten and cobalt were synthesized and evaluated. Their activity and stability was screened with rotating disk electrode (RDE) measurements, and this was followed by testing the down-selected cathode materials with most promising activity and stability either in PEM electrolyzer (tungsten based catalyst) or bipolar membrane electrolyzer (cobalt based catalyst). Test protocols for the electrochemical activity and durability measurements in RDE as well as pass/fail criteria for catalyst transfer to WP5 (cell assembly and cell testing) were defined in WP2 (Technical Specifications, Cost Analysis & Life Cycle Analysis, and reported in Deliverable 2.1). Stability of the most promising catalyst was scrutinized in a prolonged electrochemical test in a PEMEL. Compared to state of art Pt/C cathodes with high PGM loading, their substitution with W- or Co-based cathodes resulted in an increase of *ca* 200-250 mV in electrolyzer cell voltage (observed both for PEM electrolyzer and bipolar membrane electrolyzer) at high current density. While this shows the practical possibility to replace PGM by non-PGM catalysts at the acidic cathodes of such electrolyzers, it also reveals that further efforts are needed to reduce the gap in HER activity with Pt.
Publishable Abstract (If different from above)	

REVISIONS			
Version	**Date**	**Changed by**	**Comments**
1.0	21.12.2020	(Aalto)	
	22.01.2021	CNRS	
	27.01.2021	CNRS	

D3.6 - CRM-FREE METAL@CARBON MATERIALS AS HER CATALYSTS: SYNTHESIS, CHARACTERIZATION AND PERFORMANCE IN BMEL

Content

1. INTRODUCTION

For the hydrogen evolution reaction (HER) occurring in acidic medium at the cathode of proton exchange membrane electrolyzer (PEMEL) or bipolar membrane electrolyzer (BMEL), the electrodes and catalysts experience potentials below 0 V_{RHE} (more or less negative, depending on their activity) during the HER. State-of-the-art catalyst utilized today in PEMEL cathodes is platinum because of its good durability in acidic media and optimal hydrogen binding energy which results in high promotion of the HER. Developing non-precious metal catalysts with high activity and stability for HER in acid media is challenging because most non-precious metals are not stable in low pH medium, and their activity is also lower than that of PGM-based materials.

The aim of Deliverable 3.6 is to identify and characterize a set of platinum group metal (PGM) free metal@carbon materials as HER catalysts, especially for use in BMEL devices where they can be combined with PGM-free anodes due to the differential pH allowed between cathode and anode with bipolar membranes. Until now, most PGM-free catalysts developped for HER have been tested in rotating disk electrode and at low current density, rather than with polymer electrolyte in electrolyzer devices.

Here, the activity and stability was screened with rotating disk electrode (RDE) measurements, and this was followed by testing the cathode materials with most promising activity and stability in PEMELs or BMELs. Test protocols for the electrochemical activity and durability measurements in RDE as well as pass/fail criteria for catalyst transfer to WP5 (cell assembly and cell testing) were defined in WP2 (Technical Specifications, Cost Analysis & Life Cycle Analysis, and reported in Deliverable 2.1). In the following, materials performances measured in RDE are reflected against these criteria.

Down-selected materials were tested in PEMEL device (without any support electrolyte) and/or in flow cell BMEL device, with flowing anolyte and catholyte to ensure a differential pH across the membrane. Stability of the most promising catalysts was scrutinized in a prolonged electrochemical test in a PEMEL.

2. Fe@C/CNT for HER in acid (AALTO)

2.1 Synthesis of Fe@C/CNTs Catalysts with a CVD method

Synthesis of PGM-free Fe@C materials for HER in acid medium was investigated with a floating catalyst chemical vapour deposition (CVD) method. The methods yields carbon nanotubes (CNTs) containing carbon-encapsulated iron nanoparticles (Fe@C) The presence of iron nanoparticles on the CNT surface has been confirmed by TEM imaging as shown in **Figure 1a**. The size of the nanoparticles was around 5 nm. While some of the particles were encapsulated by several carbon layers, some seemed to be encapsulated by one layer only, or even exposed. XPS analysis of the Fe 2p region confirmed that the Fe particles were present as Fe^0, **Figure 1b**, suggesting full encapsulation in carbon layers as Fe is otherwise readily oxidized in air. Optimization of the synthesis conditions such as temperature, material growth catalysing ferrocene concentration, sulphur co-catalyst concentration, carbon source feed and carrier gas H_2 flow rate, was studied to improve the catalytic activity of Fe@C/CNTs towards the HER.

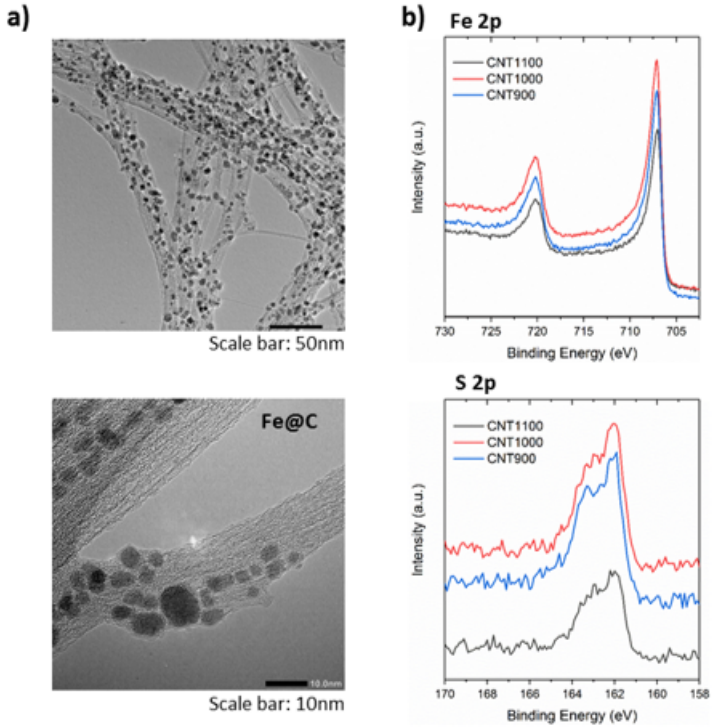

Figure.1. Characterization of Fe@C/CNTs. a) *TEM images of Fe@C/CNT synthesized at 900°C.* ***b)*** *XPS of the Fe 2p and S 2p regions for Fe@C synthesized at different temperatures in 6.5L/min H_2*

2.2 Electrochemical Activity

The synthesis temperature of 900°C resulted in a Fe@C electrocatalysts with a higher HER activity compared to its counterparts prepared at 1000°C and 1100°C. Furthermore, increasing the amount of ferrocene in the liquid precursor increases the synthesis yields, but did not affect the electrocatalytic activity. No effect on the HER activity could be observed when altering the amount of sulfur and carbon in the synthesis precursors. High flow rates of the carrier gas H_2 during synthesis was found to be crucial for obtaining active Fe@C catalysts. **Figure 2** shows the polarization curve for HER in 0.5 M H_2SO_4 for Fe@C synthesized with two different H_2 flow rates. Increasing the flow rate from 6.5L/min to 7.2L/min considerably increased the HER activity of the obtained Fe@C materials. Nevertheless, the most active materials showed clearly worse performance compared to target values listed in **Deliverable 2.1**.

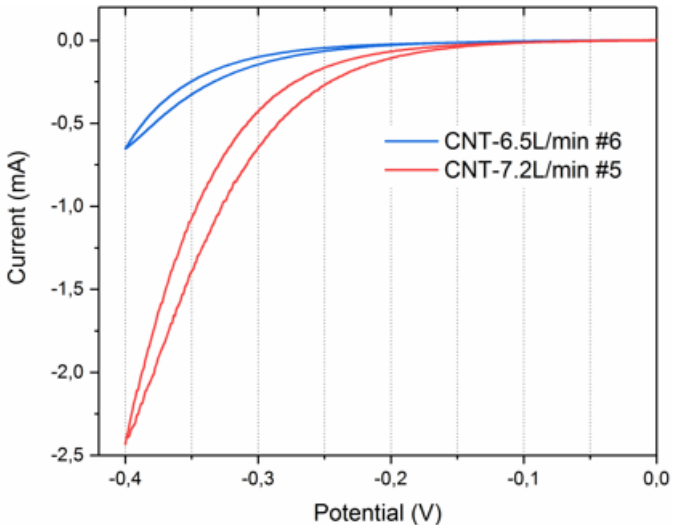

Figure.2. HER activity of Fe@C/CNTs synthesized with different H_2 flow rate during CVD. *HER was measured in H_2 saturated 0.5M H_2SO_4 at 2500 rpm with a scan rate of 2 mV s^{-1} (no iR correction). Working electrode (WE): catalysts on glassy carbon, counter electrode (CE):IrO_2, reference electrode (RE): reversible hydrogen electrode (RHE).*

2.3 Conclusions and comparison to internal CREATE Targets

Electrocatalytic activity of Fe@C towards HER activity can be improved by optimizing the CVD synthesis conditions. However, even the most active materials did not meet the CREATE activity targets.

3. Fe@C, Ni@C and FeNi@C for HER in Acid (AALTO)

3.1 Synthesis of Fe@C, Ni@C and FeNi@C Catalysts with a PLD method

The synthesis of Fe@C, Ni@C and FeNi@C was investigated using a pulsed laser ablation method (PLD) where a transition metal target is immersed in a solvent and heated with a laser to liberate nanoparticles [1]. For this process, an Nd: YAG laser with a wavelength of 1064 nm, pulse energy of 95 µJ, a pulse duration of 10 ps and a repetition rate of 100 kHz was used. For synthesizing the nanoparticles (NPs), a Ni, Fe or NiFe target was placed in a stirred aluminium batch chamber filled with the selected solvent and the ablation was carried out. The effect of laser pulse length, solvent (acetone, ethanol, toluene, water) and metal target composition was investigated to improve the material activity towards the HER.

The selection of the solvent and the transition metal target both affected the carbon shell thicknesses and the chemical nature of the transition metal cores. This was attributed to different tendency of the transition metals to form carbides and the relative amount of carbon in the solvents. In case the NPs were encapsulated in carbon shells, transition metal cores with different ratios of metallic and carbide phase were obtained. Those NPs which had incomplete or no carbon shell (in case of using water as solvent in the PLD synthesis) had also oxides in the transition metal core. In general, the mean NP diameters were around 10 nm (**Figure 3**) and for the materials synthetized in organic solvents the carbon layer thicknesses varied from incomplete to few layers and up to several nm thick encapsulations layers.

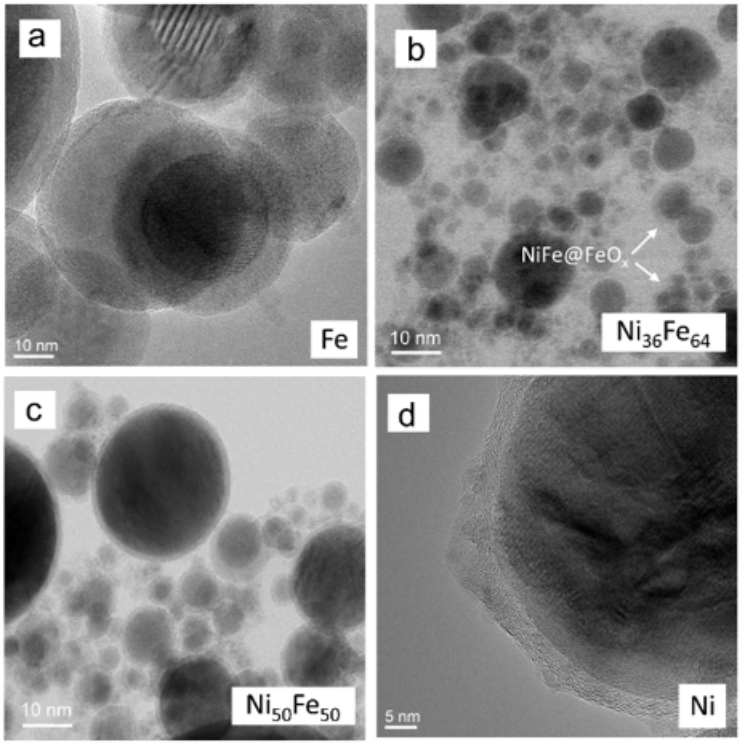

Figure.3 HR-TEM images of metal@carbon nanoparticles synthesized from (a) Fe, (b) $Ni_{34}Fe_{64}$, (c) $Ni_{50}Fe_{50}$ and (d) Ni foils with a ps-laser in acetone [1].

3.2 Electrochemical Activity and Stability

The activities of the materials were evaluated with an RDE setup in H_2-saturated 0.5 M H_2SO_4 solution (**Figure 4a**). Based on the linear sweep voltammetry measurements, the highest HER activity is achieved with $Ni_{80}Fe_{20}$@C with diameter of ~12 nm. This material has a transition metal core, comprising

a mixture of NiFe alloy and Ni_3C. The core is encapsulated in few (1-4) graphitic carbon layers. With this material HER activity of 2.1 mA/cm^2 @ -0.2 V_{RHE} is achieved, which is still significantly below the CREATE activity target of 2.2 mA/cm^2 @ -0.05 V_{RHE}. The better performance compared to the other studied PLD synthetized material is attributed to the thinner carbon shell of $Ni_{80}Fe_{20}$@C. Based on our experimental and theoretical investigations [1, 2] metal atoms are needed to activate the carbon shell and this can only take place if the carbon shell is thin enough and/or some transition metal atoms are located inside the carbon shell itself.

The material showing the highest HER activity was selected for a stability test and the results are shown **Figure 4b**. The stability measurement, carried out following a modified AST9 protocol as defined in Deliverable D2.1 of CREATE, showed excellent stability. However, the activity was still low compared to state-of-art Pt/C materials and $Ni_{80}Fe_{20}$@C was not selected for further electrolyzer testing.

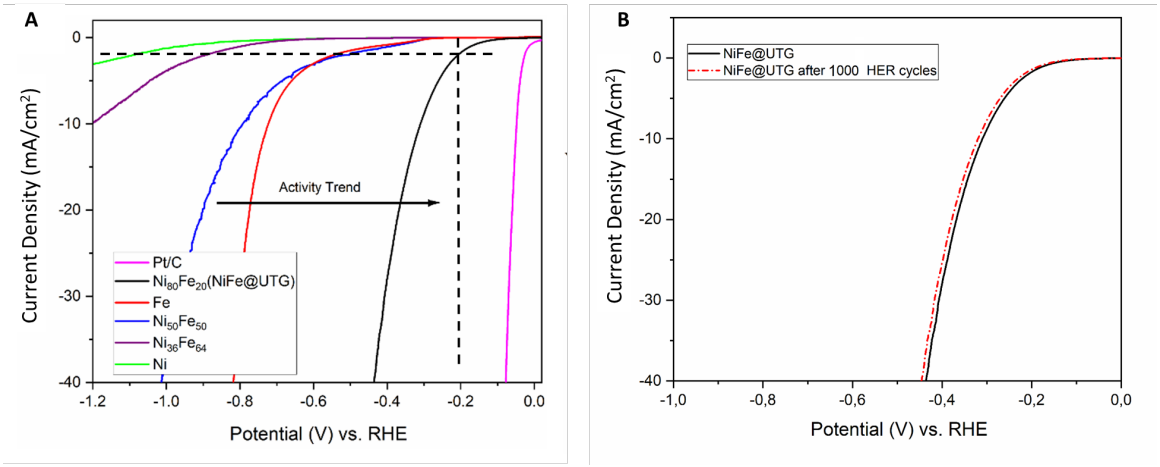

Figure 4. HER activity of metal@carbon samples. a) *HER polarization curves of samples with different cores: Fe, $Ni_{36}Fe_{64}$, $Ni_{50}Fe_{50}$, $Ni_{80}Fe_{20}$ and Ni (produced in acetone with ps-laser) in comparison to commercial Pt/C catalyst. Measured in H_2 saturated 0.5 M H_2SO_4 at 2500 rpm with a scan rate of 10 mV s^{-1} and a catalyst loading of 200 $\mu g/cm^2$ and* ***b)*** *stability test for the $Ni_{80}Fe_{20}$@C electrocatalyst showing the highest HER promotion ability [1]. Data is not iR corrected.*

3.3 Conclusions and comparison to internal CREATE Targets

The structure and electrocatalytic activities of PLD synthetized transition metal core – carbon shell NPs varied depending on the synthesis conditions. Among the studied material, the $Ni_{80}Fe_{20}$@C NPs with a thin carbon encapsulations layer showed the best performance and excellent stability suggesting that that the carbon shell can protect the transition metal core. Yet, its HER promotion ability was below the CREATE activity targets.

4. Fe/CNTs for HER in acid (Aalto)

4.1 Synthesis of Fe/CNTs Catalysts with ALD method

The catalysts were synthesized by depositing Fe precursor on CNTs by an atomic layer deposition (ALD) method and annealing at different temperatures. The samples are named with the annealing temperatures, i.e. Fe/CNTs-600, Fe/CNTs-700 and Fe/CNTs-800.

As the XRD data shows in **Figure 5**, the CNTs original structure (wide peaks before 40°) was changed after the ALD process. Moreover, the intensity of peak at 44.7° increased, which indicates that the Fe precursor was successfully deposited on CNTs. However, the peak at 44.7° almost disappeared after annealing suggesting loss of some Fe atoms during the annealing which is attributed to the low sublimation temperature of the Fe precursor. These result suggest that the Fe loading on CNTs could be increase in the future either by increasing the sublimation temperature of Fe precursors or by decreasing the annealing temperature.

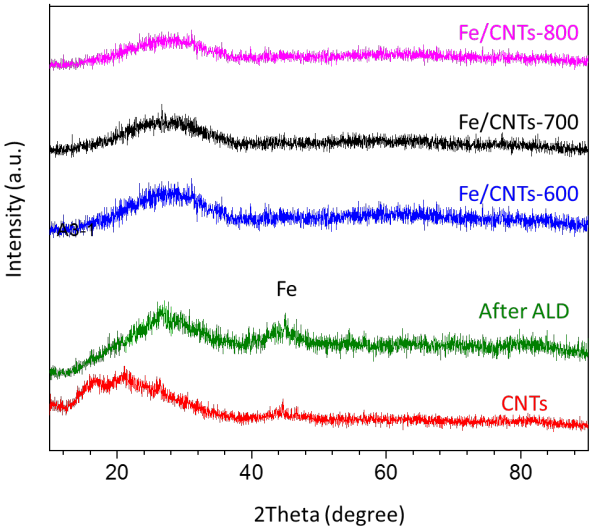

Figure 5. XRD of the samples after each step in synthesis.

The metal loss of the annealing process is also reflected by the SEM-EDS data in **Figure 6** showing the Fe content decrease from about 2 wt.% after ALD to <1 wt.% after annealing. Although the Fe content after ALD is the highest among the samples, large Fe particles are not observed in the TEM images shown in **Figure 6**, which indicates that Fe is well distributed on CNTs. However, annealing induces Fe aggregation as Fe containing particles can be observed in all TEM images of Fe/CNTs-600, Fe/CNTs-700 and Fe/CNTs-800.

4.2 Electrochemical Activity and Stability

The activity of the materials was evaluated with a RDE setup in H_2 saturated 0.5 M H_2SO_4 (**Figure 7**). As shown in **Figure 7A**, among the Fe based catalysts, Fe/CNTs-600 displays the best performance. Hence, the stability of Fe/CNTs-600 was evaluated with the stability test AST-9 in N_2 saturated 0.5 M H_2SO_4, in accordance to CREATE **Deliverable 2.1**. As shown in **Figure 7B**, the difference before and after AST9 is acceptable according to the pass/fail criteria for catalysts defined in WP2 (D2.1). The decrease in Fe/CNTs-600's performance from **Figure 7A** to **Figure 7B** indicates that the catalyst is not stable in isopropanol dispersion (the time interval is about one month between the tests).

Fe/CNTs before heating			Fe/CNTs-600			Fe/CNTs-700			Fe/CNTs-800		
Element	Wt.%	At.%	Element	Wt.%	At.%	Element	Wt.%	At.%	Element	Wt.%	At.%
C	90.5	97.8	C	95.9	99.1	C	97.8	99.5	C	95.6	99.0
Fe	9.5	2.2	Fe	4.1	0.9	Fe	2.2	0.5	Fe	4.4	1.0
Total	100	100	Total	100	100	Total	100	100	Total	100	100

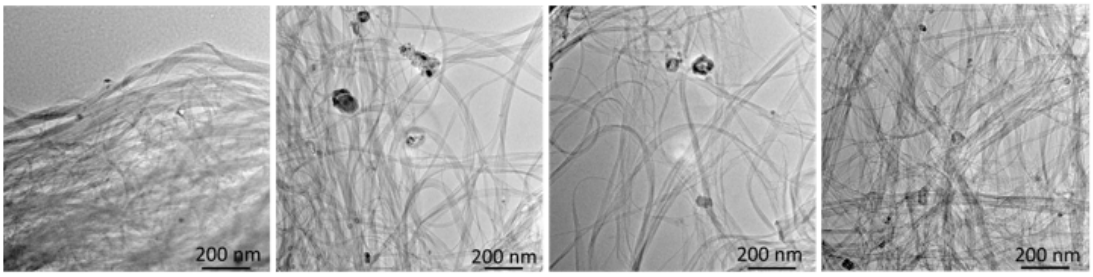

Figure 6. SEM-EDS data and TEM data of all the samples after ALD and annealing at different temperatures

When increasing the loading of Fe/CNTs-600 on the glassy carbon disk or increasing the temperature, the performance was improved, as shown in **Figure 7C** and **Figure 7D**. However, the onset potentials still remain around -200 mV_{RHE} even after increasing the loading and temperature, which is clearly worse performance compared to target values defined in Deliverable 2.1, so the electrolyser performance was not tested.

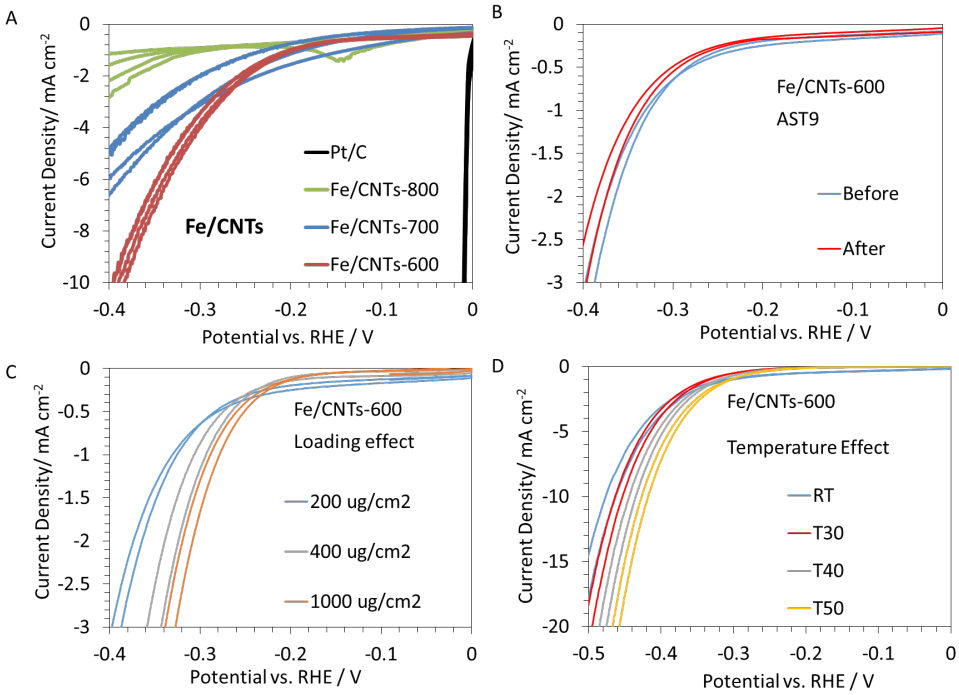

Figure 7. HER activity in H_2 saturated 0.5M H_2SO_4. A. *HER performance of Fe/CNTs-600, Fe/CNTs-700 and Fe/CNTs-800 compared with commercial 40% Pt/C catalyst. Pt/C loading is 160 μg/cm². Other catalysts' loading is 200 μg/cm². **B.** HER performance of Fe/CNTs-600 before and after AST-9. **C.** Loading effect of Fe/CNTs-600. **D.** Temperature effect of Fe/CNTs-600. WE: catalysts on glassy carbon, CE: graphite rod. Scan rate 2 mV/s, rotation speed 2500 rpm. All the data are iR corrected.*

4.3 Conclusions and comparison to internal CREATE Targets

In conclusion, with the ALD method, the best Fe/CNTs sample achieved -2 mA/cm² at about -0.2 V V_{RHE} , which is significantly below the CREATE activity target of 2.2 mA/cm² @ -0.05 V_{RHE}.

5. W_xC/CNTs FOR HER IN ACID (AALTO)

5.1 Synthesis of W_xC/CNTs Catalysts

First, WO_3 powder was synthesized by a hydrothermal reaction. Then the WO_3 powder was reduced and carbonized by melamine at high temperature in N_2 atmosphere. The resulting powder was characterized with XRD. According to the XRD pattern in **Figure 8**, the powder is a mixture of WC (PDF#51-0939) and W_2C (PDF#35-0776), so the powder is marked as W_xC ($1<x<2$). From the width of the peak for WC (101 facet), the average crystal size is estimated to be around 11 nm. From the width of the peak for W_2C (101 facet), the average crystal size is estimated to be around 47 nm. Hence, according to XRD pattern, the powder appears to be a mixture of WC small nanoparticles and W_2C large nanoparticles.

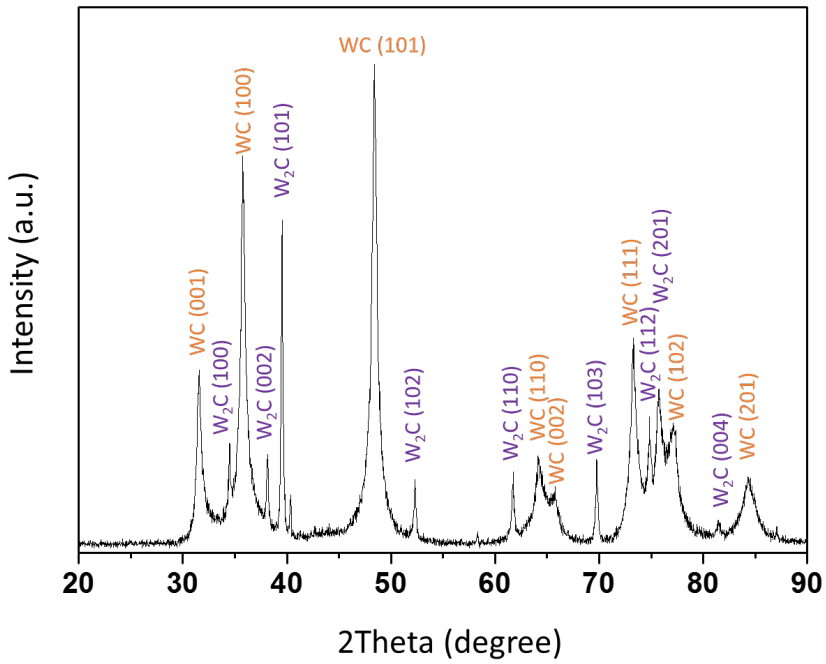

Figure 8. XRD of tungsten carbides

In accordance with the XRD pattern, nanoparticles can be seen in SEM (**Figure 9A-B**) and TEM images (**Figure 9D** and **Figure 9E**). The nanoparticles aggregate into secondary micro-particles, as shown in **Figure 9A**. From the SEM-EDS data in **Figure 9C**, the mass ratio of WC and W_xC can be estimated as 3:2. The larger ratio of WC compared to W_xC is reflected in the XRD pattern (**Figure 8**) showing more intense WC peaks, though the difference is small. To improve the conductivity, W_xC was mixed with CNTs in isopropanol dispersion. The share of CNTs in W_xC/CNTs is 10 wt. % and CNTs were pre-treated with HCl before using. As shown in **Figure 9F**, the W_xC particles are tightly connected in the net of CNTs.

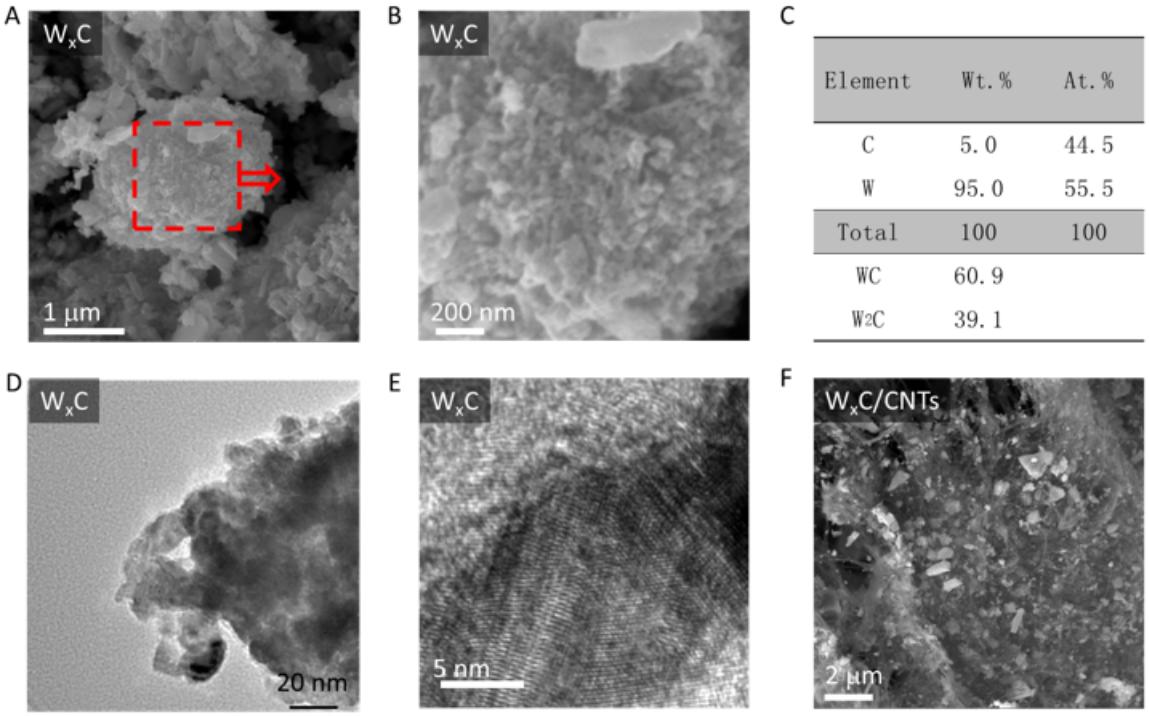

Element	Wt.%	At.%
C	5.0	44.5
W	95.0	55.5
Total	100	100
WC	60.9	
W_2C	39.1	

Figure 9. SEM and TEM characterization. A and B, SEM images of W_xC and C the SEM-EDS data. D and E, TEM images of W_xC. FSEM image of the mixture of W_xC (90 wt. %) and CNTs (10 wt. %).

5.2 Electrochemical Activity and Stability

The activity of the materials was evaluated with an RDE setup in H_2 saturated 0.5M H_2SO_4 (**Figure 10**). As shown in **Figure 10A**, the HER performance was very slightly improved by adding CNTs into W_xC. Then the stability of W_xC/CNTs was evaluated by the stability test AST-9 in N_2 saturated 0.5M H_2SO_4, in accordance to CREATE **Deliverable 2.1**. As shown in **Figure 10B**, the difference before and after AST-9 is acceptable. Before the PEM electrolyzer test, the temperature effect on W_xC/CNTs and loading effect on W_xC were measured. As shown in **Figure 10C** and **Figure 10D**, both increased temperature and increased loading could improve the performance, so it is reasonable to use the higher temperature and higher loading for further electrolyzer tests.

The electrolyzer measurements (**Figure 11**) were conducted with IrO_2 anodes and Nafion 115 membranes at 50°C. For these tests, PEMEL setup was selected since the cathode environment is acidic, as in the intended BMEL, and PEMEL is a robust technology while bipolar membranes are still at low TRL. The loadings of carbon, commercial 40 wt. % Pt/C, IrO_2, W_xC and W_xC/CNTs were targeted at 0.75 mg/cm^2, 1.25 mg/cm^2, 2.3 mg/cm^2, 12.5 mg/cm^2 and 13.9 mg/cm^2, respectively. However, due to the spray efficiency of the inks, the loadings fluctuate around the target level.

The trend in **Figure 11A** is quite similar with the data in **Figure 10**: Pt/C exhibits the highest performance according to polarization curves and W_xC/CNTs exhibits somewhat higher current densities than W_xC. Due to higher loadings of W_xC and W_xC/CNTs than that of Pt/C in **Figure 11A**, the difference of the curves becomes smaller than in **Figure 10A**. At the current density of 0.4 A/cm^2, the voltage needed for W_xC/CNTs is only ~220 mV larger than for Pt/C. Although the price of Pt is about 970 times higher than W due to the scarcity of Pt, W is also listed as a CRM by the EU [3]. However, its supply risk is recognized as low and hence it can be considered a reasonable alternative to Pt.

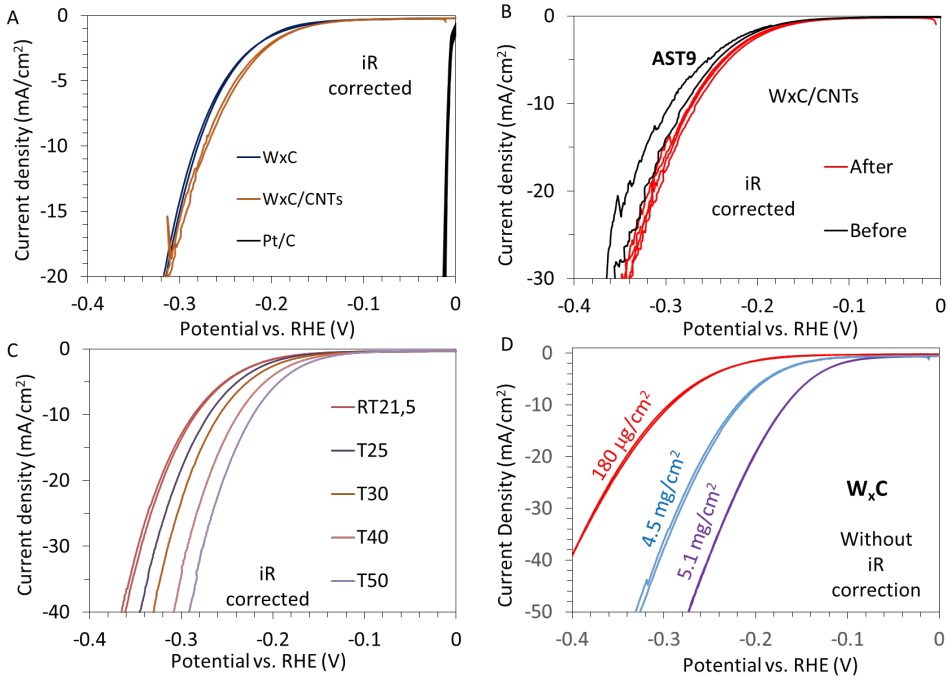

Figure 10. HER activity in H_2 saturated 0.5M H_2SO_4. A. *HER performance of W_xC and W_xC/CNTs in comparison with commercial 40% Pt/C catalyst. Pt/C loading is 160 µg/cm². W_xC loading is 180 µg/cm², W_xC loading is 180 W_xC + 20 CNTs µg/cm². **B.** HER performance of W_xC before and after AST9. **C.** Temperature effect on W_xC/CNTs. **D.** Loading effect of W_xC. WE: catalysts on glassy carbon, CE: graphite rod. RE: Hg/Hg_2Cl_2. Scan rate 2 mV/s, rotation speed 2500 rpm. The current densities are normalized with geometric surface area*

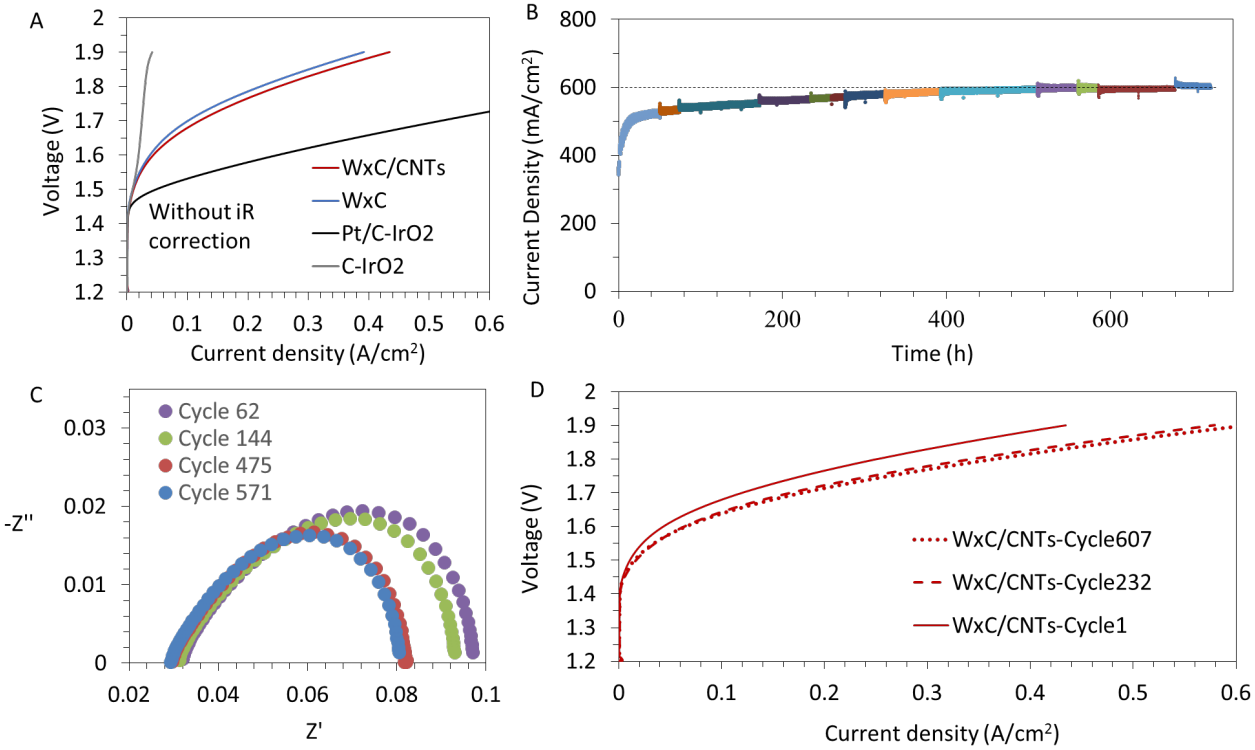

Figure 11. Electrolyzer measurements. A. *Comparison between C, Pt/C, W_xC and W_xC/CNTs in an electrolyzer. **B.** Stability test of W_xC/CNTs-IrO_2 at 1.9 V. 608 on and off cycles (1h on per cycle) were recorded and after each cycle LSVs were tested. The time for LSV tests are included in the total time. **C.** Impedance change during stability test. **D.** LSV curves change during the stability test. The electrolyzer data were not iR corrected.*

The startup - shut down stability test in the electrolyzer was conducted by polarizing the cell voltage to 1.9 V. For each start – stop cycle, the cell was on for 1 h and off for 15 min. As shown in **Figure 11B**, the performance increases obviously during 400 h reflecting the decrease in the cell impedance (**Figure 11D**) and reaches a stable current density of about 600 mA/cm^2. In **Figure 11D** polarization curves show the performance improvement: from Cycle1 to Cycle232, the performance increases notably; from Cycle232 to Cycle607, there is no obvious change.

5.3 Conclusions and comparison to internal CREATE Targets

In conclusion, the mix of CNTs into W_xC increased the performance and the material start up and shut down stability is excellent among reported articles, as shown in **Table 2**. However, W_xC/CNTs achieved an HER activity at -2 mA/cm^2 of about -0.2 V_{RHE}, which is clearly below the CREATE activity target of 2.2 mA/cm^2 @ -0.05 V_{RHE}.

6. Co_5NC FOR HER IN ACID (CNRS)

6.1 Synthesis of Co_5-NC Catalyst

The catalyst was a cobalt-based material comprising metallic cobalt particles surrounded by a graphite layer. The preparation route is based on pyrolysis of ZIF-8. In this route, among 3d transition metals, the highest activity is not reached with Fe but with cobalt.[12] While cobalt belongs to the current list of critical raw materials (CRMs) as defined by the European Union, it is much more abundant than any of the PGMs, and its use in BMEL would represent a minimal share of the global yearly production of cobalt. The cobalt-NC catalyst precursor was prepared by combining the Zn(II) zeolitic imidazolate framework ZIF-8 (Basolite Z1200, labelled ZIF-8), furfuryl alcohol (FA), cobaltous acetate, and 1,10-phenanthroline (phen). ZIF-8 was first impregnated with FA, using 4 mL of FA per gram of ZIF-8. The resultant mixture was stirred for 24 h, filtered and washed with mesitylene to remove excess FA. We then prepared the Co/phen/Z8FA catalyst precursors of weight compositions 5/20/80. The scalar of 5 stands for 5 wt. % of cobalt) in the catalyst precursor, while 20/80 is the mass ratio of phen to the microporous host Z8FA. The suspension was stirred 2 h, then slowly evaporated and dried overnight at 80 °C. The resulting powder was subjected to planetary ball-milling to form the catalyst precursor. One gram of catalyst precursor was ball-milled in a zirconium oxide crucible filled with zirconium oxide balls. The vial was sealed under air and placed in a planetary ball-miller. The catalyst precursor collected after ballmilling then underwent a pyrolysis in flowing Ar at 1050 ºC for 1 h, with a heating in ramp mode (5 ºC·min^{-1}). The resulting catalyst is labelled $Co_{5.0}$-NC. Due to important loss of Zn, C and N elements from the catalyst precursor during pyrolysis (forming volatile products), the cobalt content in the final catalyst is multiplied by *ca* three-fold, resulting in Co bulk content of *ca* 15 wt% in $Co_{5.0}$-NC. Metallic particles with size in the range of 10-30 nm are observed in in $Co_{5.0}$-NC, and identified by XRD to be metallic cobalt (**Figure 12**). Its BET area is *ca* 510 m^2/g (micro and mesoporous), mostly assigned to the carbon area.

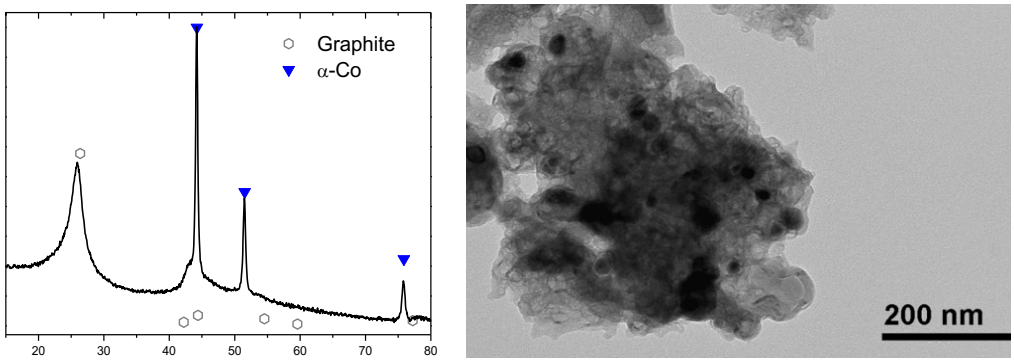

Figure 12. *X-ray diffraction pattern for $Co_{5.0}$-NC catalyst, identifying graphite and metallic cobalt; and TEM image of $Co_{5.0}$-NC showing metallic cobalt particles surrounded by carbon/graphite shell.*

6.2 Electrocatalytic activity of $Co_{5.0}$-NC Catalyst

The HER activity in acid medium of $Co_{5.0}$-NC was verified with rotating disk electrode method and showed at a low catalyst loading of 0.2 mg cm^{-2} overpotentials of *ca* 260 mV at -2 mA·cm^{-2} (**Figure 13**). This HER activity is comparable although somewhat lower (by 40-60 mV at -2 mA·cm^{-2}) than that of the best PGM-free materials reported in sections 2-4 above.

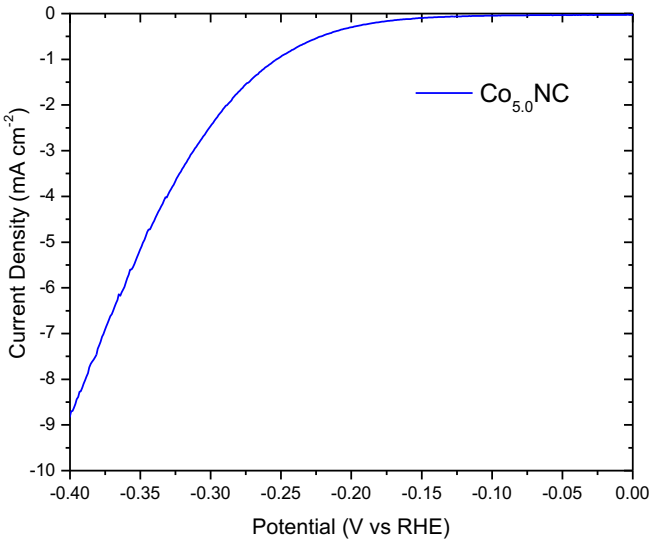

Figure 13. *HER activity in acid of $Co_{5.0}$-NC. The electrolyte was 0.5 M H_2SO_4, the rotation 1600 rpm, scan rate 1 mV·s^{-1} and catalyst loading 0.2 mg·cm^{-2}.*

Then, a BMEL test was performed with $Co_{5.0}$-NC at the cathode, paired with a PGM-free anode (developped by ICIQ) and a bipolar membrane (developped by Fumatech in WP4). The anode and bipolar membrane are described in detail in the public deliverable D4.5 of CREATE. The $Co_{5.0}$NC cathode was prepared as follows: Cathode ink was prepared by mixing 20 mg of $Co_{5.0}$NC with 652 µL of 5 wt% Nafion solution containing 15-20 % water, 326 µl of ethanol and 272 µl of de-ionized water. The ink solution was then ultrasonicated for 1 h before being drop cast on an 18 cm^2 gas diffusion layer (Sigracet 39BC).

The anode, BM and cathode were installed in a commercial Micro Flow Cell (MFC) purchased from ElectroCell. The electrochemical surface area is 10 cm^2. Current densities reported were normalized by the geometric surface area (10 cm^2). All tests were performed at atmospheric pressure and room temperature. The thickness of liquid anolyte and catholyte is *ca* 3 mm each. Anolyte and catholyte were recirculated with a peristaltic pump in the reservoir of 200 or 250 mL at a flow rate of 100 mL/min. The gap between the membrane separating the two electrolyte compartments and each electrode is *ca* 3-5 mm, depending on the gasket and compression. For all tests 5 Nm of torque was applied to each bolt. For the tests, 1.0 M KOH and 0.5 M H_2SO_4 was used as anolyte and catholyte, respectively. The linear scan amperometry was performed at 1 mA·cm^{-2}·s^{-1} by scanning the cell current density from 0 to 450 mA·cm^{-2}. Afterwards, the galvanostatic measurements were performed for 5 min at each of the following current densities: 0.5, 1.5, 20, 45, 100, 200 and 450 mA·cm^{-2}.

Figure 14 shows that switching from Pt to a Co-based cathode in BMEL leads to an increase of *ca* 250 mV in cell voltage (compare blue vs. green curve), in line with onset potential for HER for $Co_{5.0}$-NC of *ca* -200 mV vs. RHE seen in RDE, and also in line with **Table 2**, reporting an increased voltage of ca 200-250 mV when switching from Pt to state-of-art PGM-free catalysts at the cathode of PEMEL.

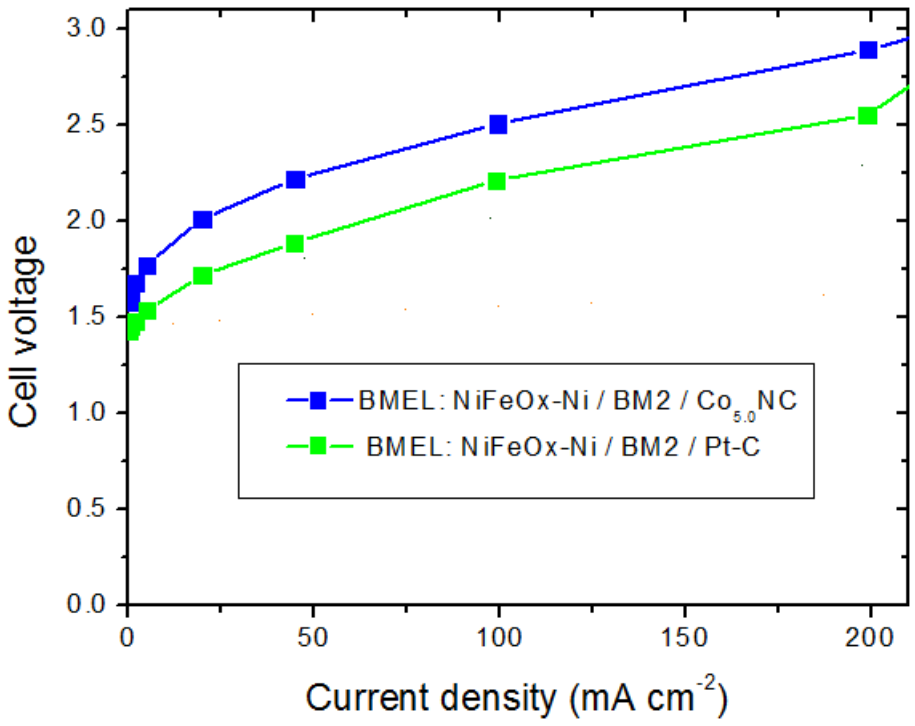

Figure 14. *Comparison of BMEL performance with a Pt/C cathode and a $Co_{5.0}$NC cathode. Polarisation curve recorded at room temperature using the bipolar membrane BM2 (see Deliverable 4.5 for information on the BM), 1M KOH and 0.5 M H_2SO_4 as anolyte and catholyte, Fe-Ni-O_x/Ni foam anode, and either a Pt/cathode with 0.2 mg_{Pt} cm^{-2} loading (green curve) or $Co_{5.0}$NC with 1 mg cm^{-2} (blue curve). The BMEL curves are iR-corrected (mostly, for the high Ohmic drop in the electrolyte due to several mm between the BM and each electrode in the flow cell setup).*

7. COMPARISON WITH THE STATE OF ART

7.1 HER in acid with CRM/PGM free catalysts

Without a Pt counter electrode (which might activate the working electrode *in situ*), in sulfuric acid, HER catalysts based on Ni or Fe are rarely reported. Hence, even though the activity of the materials studied for Deliverable 3.6 is not equivalent compared with other non-precious metal catalysts, as shown in **Table 1**, it has special significance for the development of CRM free catalysts in the EU.

Table 1. Performance comparison of the current work and representative CRM/PGM free catalysts for HER in sulfuric acid.

Ref	Catalyst	$\eta\|10\ mA/cm^2$
This work	Fe@C/CNTs	< - 400 mV
	FeNi@C	~ -300 mV
	Fe/CNTs	~ - 400 mV
	W_xC/CNTs	~ - 285 mV
Ref4	GO@Ni	~ - 83.2 mV
Ref5	W1Mo1-NG	~ - 24 mV

7.2 PGM free catalysts for PEMEL cathode

Although many PGM free catalysts have been reported for the HER, the PEMEL performance was reported only for few of them. The representative works are listed in Table 2 showing that with the WxC/CNT anode, a promising performance and durability is achieved.

Table 2. Performance comparison of the current work and representative CRM/PGM free catalysts for PEMEL.

Ref	Cathode	Reference Cathode material	Voltage Difference with the reference			Temperature / °C	Stability		
			100 mA cm^{-2}	200 mA cm^{-2}	400 mA cm^{-2}		A	V	h
This work	W_xC/CNTs	40% Pt/C	0.149	0.187	0.225	50	0.4→0.6	1.9	608
Ref6	MoS_2/Vulcan®	Pt black	0.19V	0.23V	N/A	80	0.27→0.36	2	18
Ref7	MoP|S-CB	20% Pt/C	0.18V	0.195V	0.225V	80	0.51→0.4	1.85	24
Ref8	MoS_2	N/A	N/A	N/A	N/A	N/A	~ 0.066	2	100
Ref9	$Co_{59}Cu_{41}$	N/A	N/A	N/A	N/A	90	1	1.96→1.88	48
Ref10	Co-MoS_2	20% Pt/C	~ 0V	~ 0.09V	~ 0.18 V	80	N/A	N/A	N/A
Ref11	Mo_3S_{13}	60% Pt/C	N/A	~ 0.22V	~ 0.24V	80	1	1.93→1.94	100

8. REFERENCES

1. F. Davodi, E. Mühlhausen, D. Settipani, E.-L. Rautama, A.-P. Honkanen, S. Huotari, G. Marzun, P. Taskinen, T. Kallio, Comprehensive Study to Design Advanced Metal-carbide@Graphene and Metal-carbide@FeOx Nanoparticles with Tunable Structure by the Laser Ablation in liquid, Journal of Colloid and Interface Science, 556 (2019) 180-192.
2. F. Davodi, G. Cilpa-Karhu, J. Sainio, H. Jiang, E. Mühlhausen, B. Göcke, K. Laasonen, T. Kallio, Atomic-Scale Immobilized Pt on Metal@Carbon with Remarkable Performance for Hydrogen Evolution Reaction in Acidic Media, submitted
3. European Commission, Critical raw materials, Internal Market, Industry, Entrepreneurship and SMEs, https://ec.europa.eu/growth/sectors/raw-materials/specific-interest/critical_en
4. Sarawutanukul S, Phattharasupakun N, Sawangphruk M. 3D CVD graphene oxide-coated Ni foam as carbo- and electro-catalyst towards hydrogen evolution reaction in acidic solution: In situ electrochemical gas chromatography. Carbon 151, 109-119 (2019).
5. Yang Y, et al. O-coordinated W-Mo dual-atom catalyst for pH-universal electrocatalytic hydrogen evolution. Science Advances 6, (2020).
6. Corrales-Sanchez T, Ampurdanes J, Urakawa A. MoS2-based materials as alternative cathode catalyst for PEM electrolysis. Int. J. Hydrog. Energy 39, 20837-20843 (2014).
7. Ng JWD, Hellstern TR, Kibsgaard J, Hinckley AC, Benck JD, Jaramillo TF. Polymer Electrolyte Membrane Electrolyzers Utilizing Non-precious Mo-based Hydrogen Evolution Catalysts. ChemSusChem 8, 3512-3519 (2015).
8. Kumar SMS, et al. Hydrothermal assisted morphology designed MoS2 material as alternative cathode catalyst for PEM electrolyser application. Int. J. Hydrog. Energy 41, 13331-13340 (2016).
9. Kim H, Park H, Oh S, Kim S-K. Facile electrochemical preparation of nonprecious Co-Cu alloy catalysts for hydrogen production in proton exchange membrane water electrolysis. International Journal of Energy Research 44, 2833-2844 (2020).
10. Mo J, et al. Transition metal atom-doped monolayer MoS2 in a proton-exchange membrane electrolyzer. Materials Today Advances 6, (2020).
11. Holzapfel PKR, et al. Fabrication of a Robust PEM Water Electrolyzer Based on Non-Noble Metal Cathode Catalyst: Mo3S13 (2-) Clusters Anchored to N-Doped Carbon Nanotubes. Small 16, (2020).
12. A. Morozan, V. Goellner, Y. Nedellec, J. Hannauer, F. Jaouen, Effect of the transition metal on Metal-nitrogen-carbon catalysts for the hydrogen evolution reaction, J. Electrochem. Soc. 162 (2015) H719